Figure S1, related to Figure 1.

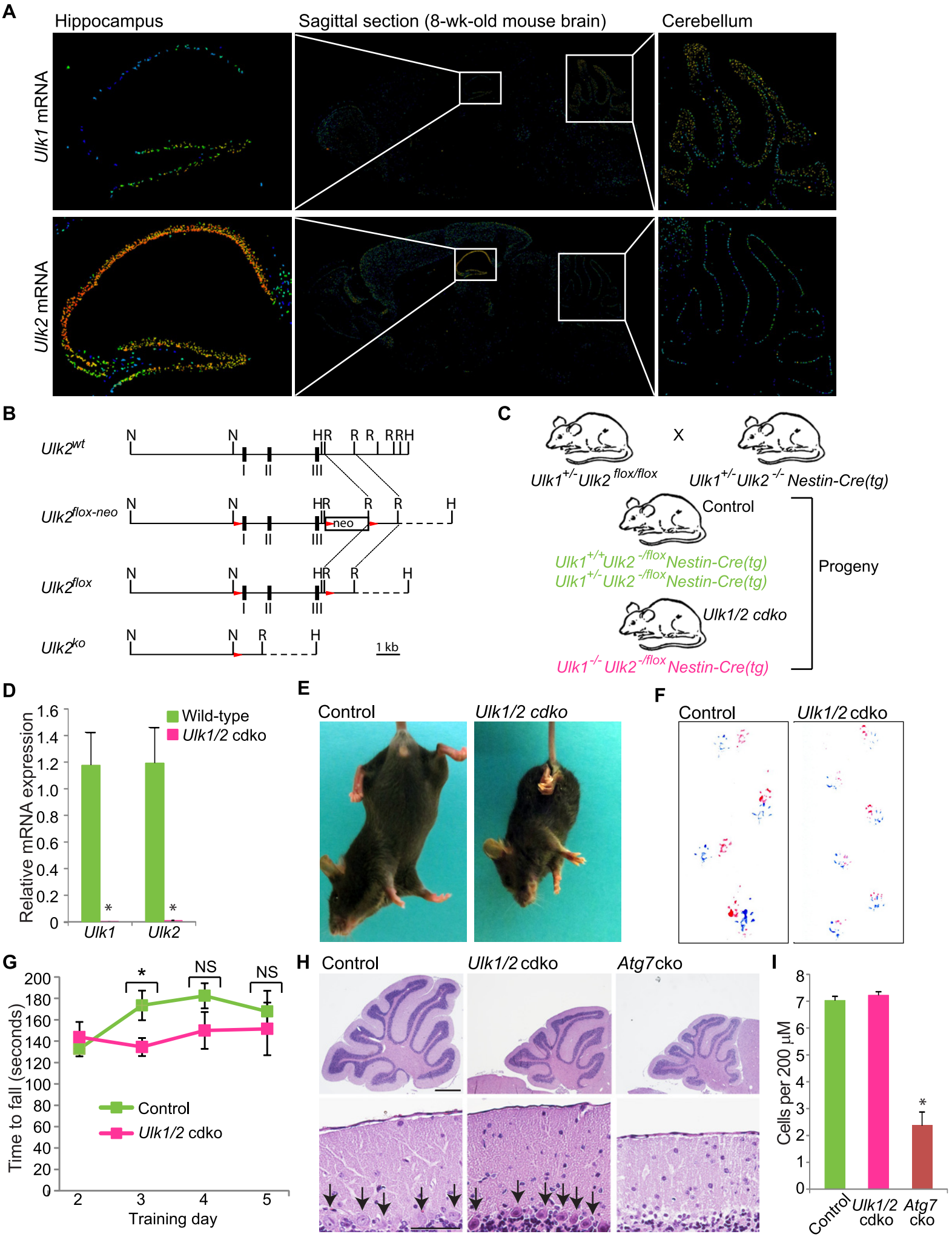

Figure S1, related to Figure 1. (A) In situ hybridization (expression density map) from the Allen Brain Atlas showing the expression of *Ulk1* and *Ulk2* mRNA in the brains of 8-wk-old mice, with magnified views of the hippocampus and cerebellum. **(B)** Genomic organization of wild-type and targeted *Ulk2* loci. The genomic organizations of the wild-type ($Ulk2^{wt}$) and targeted ($Ulk2^{flox\text{-}neo}$) *Ulk2* loci are shown (top 2 diagrams). Mice harboring the targeted *Ulk2* allele ($Ulk2^{flox\text{-}neo}$) were crossed with *EIIa-Cre* transgenic (tg) mice, and progeny harboring $Ulk2^{ko}$ or $Ulk2^{flox}$ alleles (bottom 2 diagrams) were back-crossed with WT mice to eliminate Cre-recombinase expression. **(C)** Diagram of the generation of *Ulk1/2*–conditional double-knockout (*Ulk1/2*-cdko) mice. $Ulk1^{+/-}$;$Ulk2^{flox/flox}$ mice were bred with $Ulk1^{+/-}$;$Ulk2^{-/-}$ *Nestin-Cre (tg)* mice to generate *Ulk1/2*-cdko [$Ulk1^{-/-}$;$Ulk2^{-/-}$ *Nestin-Cre* (*tg*)] mice. Controls used in the experiments included $Ulk1^{+/-}$;$Ulk2^{-/flox}$ *Nestin-Cre (tg)* and $Ulk1^{+/+}Ulk2^{-/flox}$ *Nestin-Cre (tg)* mice. **(D)** The deletion of *Ulk1* and *Ulk2* in the cdko mice was verified by RT-qPCR. The levels of *Ulk1* and *Ulk2* mRNA in the hippocampus of 8-wk-old *Ulk1/2*-cdko mice ($n = 3$) were normalized to wild-type, age-matched controls ($n = 2$). *$P < 0.001$ (Student's *t*-test). **(E)** Abnormal limb-clasping reflexes in an 8-wk-old *Ulk1/2*-cdko mouse (right photograph). When lifted by their tails and slowly lowered toward a horizontal surface, control mice (left photograph) extend their hind limbs and bodies in anticipation of contact. In contrast, *Ulk1/2*-cdko mice show a pathologic reflex, clasping their fore and hind limbs. **(F)** The ink paw-print test, in which the forepaws were marked in blue ink and the hind paws in red ink, revealed normal gait patterns in control and *Ulk1/2*-cdko mice. **(G)** Motor coordination was tested using a rotarod assay. Control ($n = 5$) and *Ulk1/2-cdko* ($n = 7$) mice were placed on a rotating rod that was accelerated from 0 to 40 rpm at a rate of 10 rpm/min, and the time spent on the rod was measured. Data shown are the means (± SEM). *$P < 0.001$ (Student's *t*-test). **(H)** Hematoxylin and eosin (H&E)-stained sections of the cerebellum in 16-wk-old control, *Ulk1*/2-cdko, and *Atg7*-cko mice demonstrate the loss of Purkinje cell neurons in the *Atg7*-cko mice. Intact Purkinje cell neurons are indicated by arrows. Scale bar: 50 μm. **(I)** The mean number (± SEM) of Purkinje cell neurons per 200 μM in 4-month-old control mice ($n = 5$), 4-month-old *Ulk1/2-cdko* mice ($n = 3$), and 2- to 4-month-old *Atg7*-cko mice ($n = 2$). *$P < 0.001$ (ANOVA).

Figure S2, related to Figure 2.

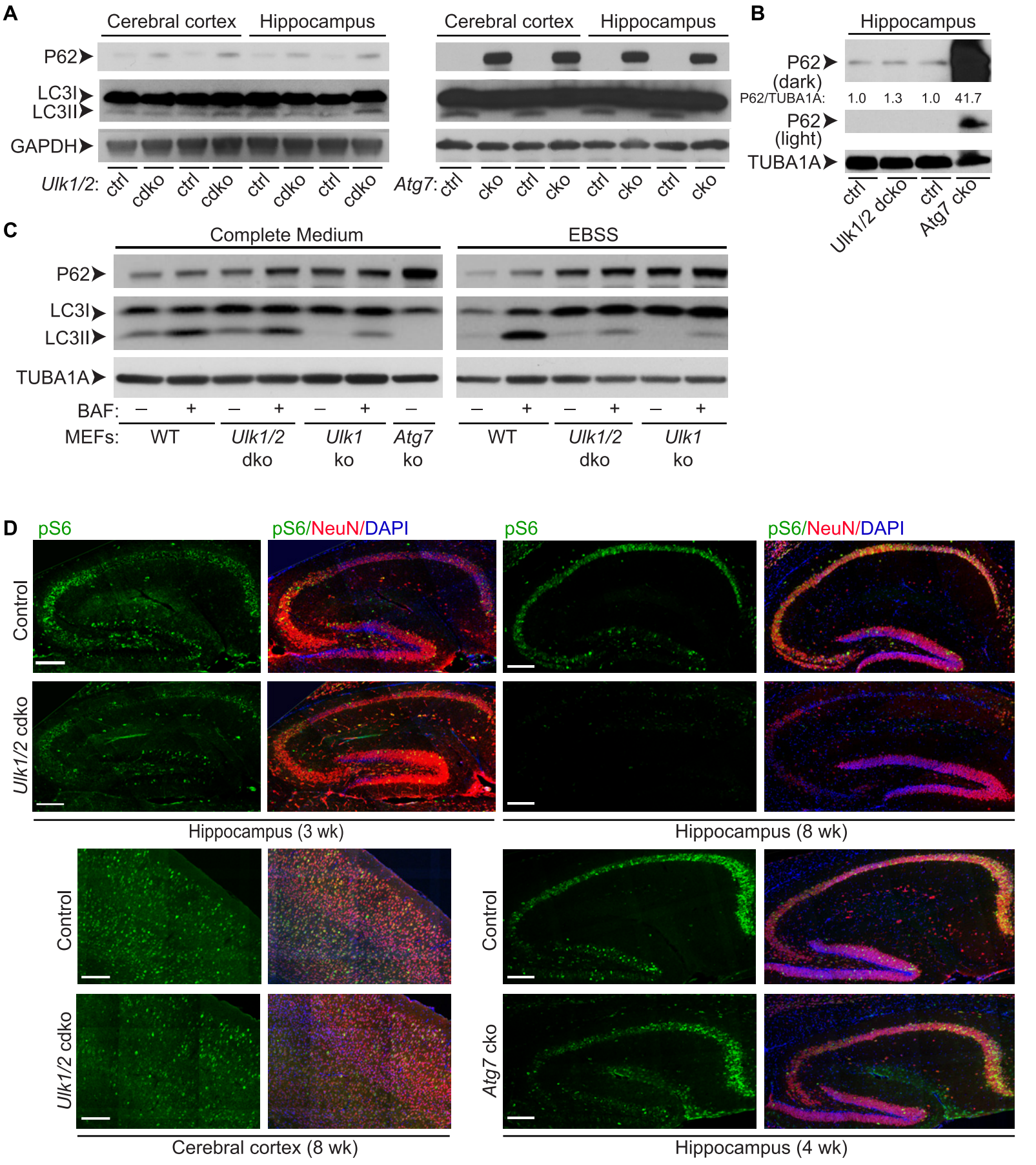

Figure S2, related to Figure 2. (A–B) Immunoblot analyses of extracts prepared from the cerebral cortex and hippocampus of 8-wk-old control (ctrl) and *Ulk1/2*-cdko mice or control (*Atg7*$^{flox/flox}$) and *Atg7*-cko mice show the dramatically increased steady-state P62 levels in *Atg7*-cko mice compared to those in *Ulk1/2*-cdko mice and littermate controls. **(C)** Extracts were prepared from WT, *Ulk1/2*-dko, *Ulk1*-ko, and *Atg7*-ko MEFs grown in complete medium or Earle's Balanced Salt Solution (EBSS) for 2 h in the presence or absence of bafilomycin A (Baf), a vacuolar type H+ ATPase that blocks lysosome-dependent protein degradation. Representative immunoblots show the increased levels of P62, along with the decreased conversion of LC3-I to LC3-II and the degradation of LC3-II in EBSS-treated *Ulk1/2*-dko and *Ulk1*-ko MEFs, consistent with a defect in starvation-induced autophagy. **(D)** Immunofluorescence microscopy of whole-brain sections from *Ulk1/2*-cdko mice, *Atg7*-cko mice, and their respective control littermates with antibodies against pS6 and NeuN. The intensity of the pS6 staining is mildly decreased in the hippocampus of 3-wk-old *Ulk1/2*-cdko mice and dramatically reduced by 8 wks. Representative images of the cerebral cortex from the same sections from 8-wk-old *Ulk1/2*-cdko and control animals are shown as positive controls for the staining. The pS6 staining in *Atg7*-cko mice is comparable to that in littermate controls. Scale bars: 200 μm.

Figure S3, related to Figure 3.

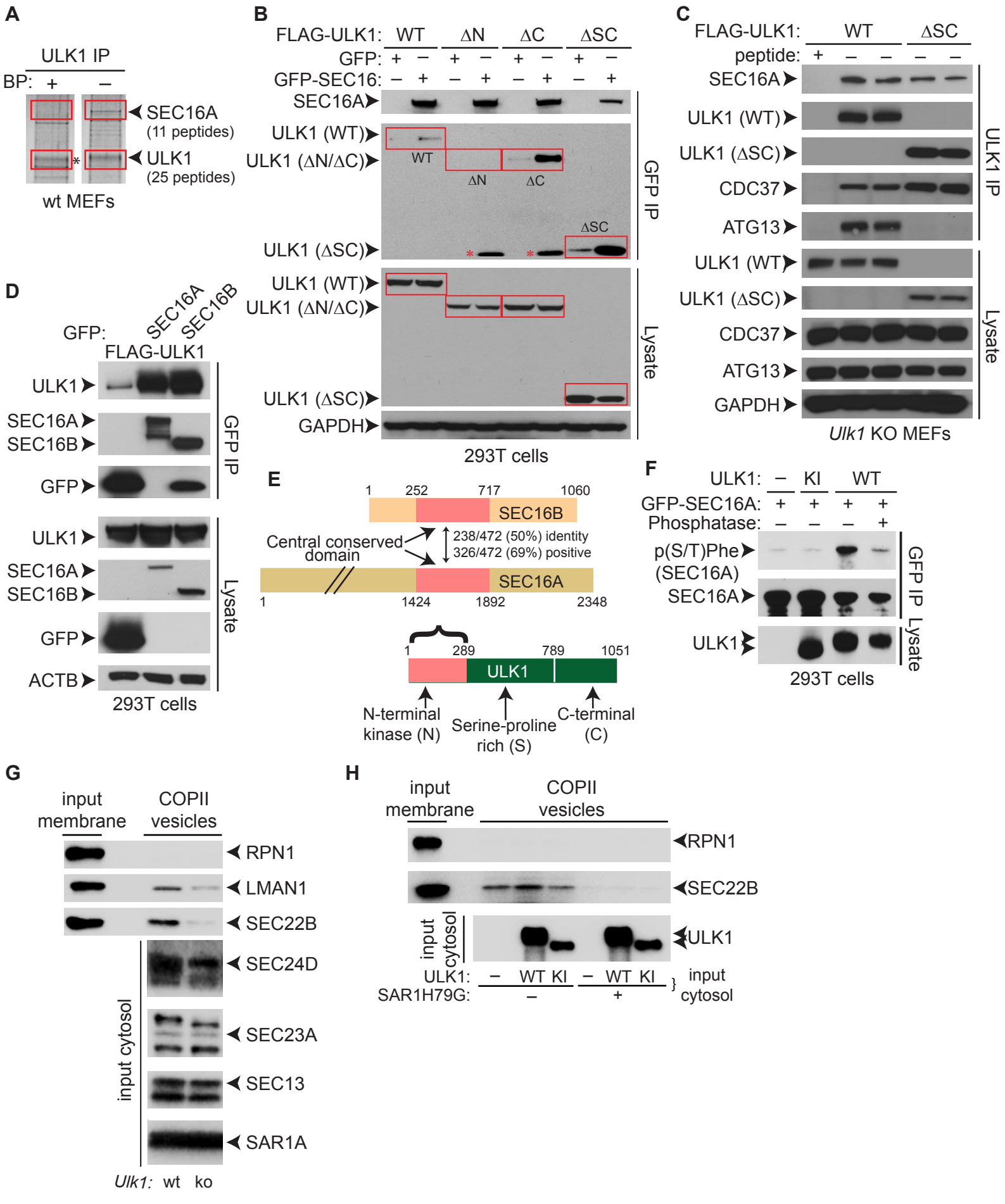

Figure S3, related to Figure 3. (A) Unbiased identification of Sec16A as an endogenous ULK1-interacting partner. Gel slices from the SYPRO Ruby–stained gel containing bands unique to endogenous ULK1^{+} immunoprecipitates (IPs) [i.e., bands not present in IPs from wild-type (WT) MEFs preincubated with blocking peptide (BP)] and corresponding regions of the control lane (outlined in red) were submitted for liquid chromatography/mass spectrometry (LC/MS) analysis. The numbers of unique peptides from SEC16A and ULK1 in the gel slices from the ULK1 IP–containing lane are indicated. The asterisk highlights a band with a migration similar to ULK1 in samples that were preincubated with BP; however, neither ULK1 nor SEC16A peptides were detected by LC/MS in the gel slices from the control lane. **(B)** GFP^{+} IPs from 293T cells transfected with N-terminal FLAG-tagged, full-length ULK1 (WT) or the indicated deletion constructs and either GFP or GFP-tagged SEC16A were subjected to immunoblot analyses. The N-terminal kinase domain of ULK1 is necessary and sufficient to mediate the interaction with SEC16A. N: N-terminal kinase domain; S: serine-proline rich "spacer" domain; C: C-terminal domain. **(C)** Immunoblot analyses of ULK1 IPs from *Ulk1*-ko MEFs stably expressing FLAG-tagged ULK1 (WT) or the N-terminal domain of ULK1 (ΔSC). **(D)** Immunoblot analyses of GFP IPs from 293T cells transfected with N-terminal FLAG-tagged ULK1 and the indicated GFP constructs (GFP alone, GFP–SEC16A, or GFP–SEC16B). **(E)** Diagram showing the homology in the central conserved domains of SEC16A and SEC16B, which most likely mediate the interaction with ULK1. The domain structure of ULK1 is also shown. **(F)** The 293T cells were transfected with GFP–SEC16A and the indicated ULK1 expression construct [i.e., WT or kinase-inactive ULK1 mutant (KI)]. GFP^{+} IPs were incubated in the presence or absence of phosphatase prior to SDS-PAGE and immunoblot analysis. **(G)** Cytosolic fractions from WT or *Ulk1*-ko MEFs and membrane fractions from WT MEFs were used in in vitro COPII-budding reactions. Immunoblot analyses demonstrate comparable levels of cytosolic COPII components in WT and *Ulk1*-ko MEFs. **(H)** Cytosolic fractions from 293T cells transfected with empty vector (−), WT, or KI ULK1 were combined with membrane fractions from untransfected 293T cells and used in the in vitro budding reaction. The ULK1-dependent increase in SEC22B incorporation into budded vesicles occurs in a SAR1 GTPase–dependent manner.

Figure S4, related to Figure 4.

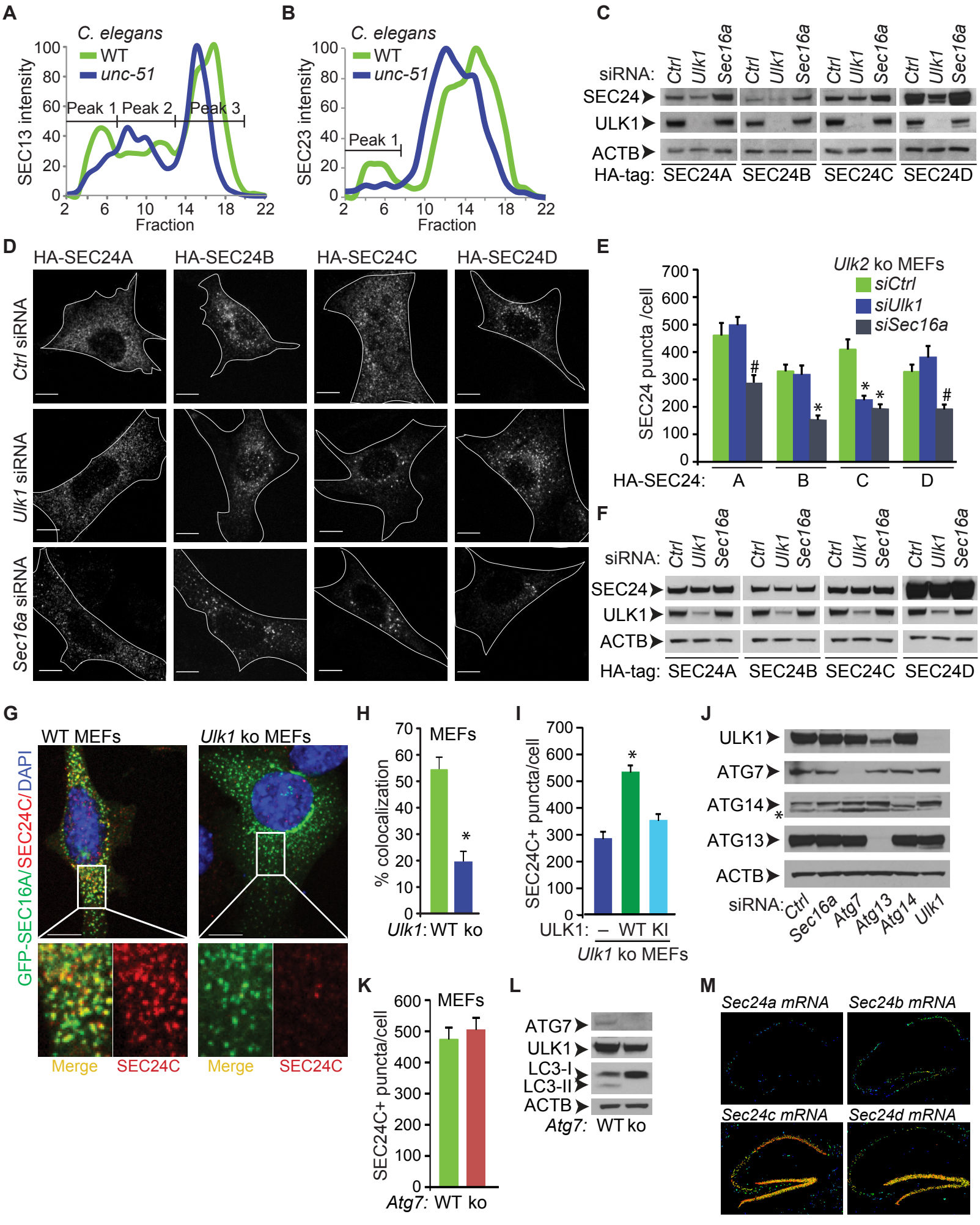

Figure S4, related to Figure 4. (A–B) Extracts prepared from WT and *unc-51*–mutant *C. elegans* were fractionated on a Superose 6 gel filtration chromatography column, and the levels of SEC13 and SEC23 in each fraction were assessed by immunoblot analysis. The intensity profiles of SEC13 and SEC23 from a representative experiment are shown in **A** and **B**, respectively. The high–molecular-weight fractions (peak 1) contain assembled COPII complexes, consisting of SEC23-containing heterodimers and SEC13-containing heterotetramers. **(C)** WT MEFs were transfected with the indicated HA-tagged SEC24 isoform (A, B, C, or D) and control nontargeting siRNA (siCtrl), Ulk1 siRNA, or Sec16a siRNA. Immunoblot analyses were performed using antibodies against the specified proteins. The decrease in SEC24C puncta in *Ulk1*-depleted cells is not associated with a decrease in the overall SEC24C protein levels. **(D)** Representative images of anti-HA–stained WT MEFs transfected with the indicated HA-tagged SEC24 isoform (A, B, C, or D) and either control nontargeting siRNA (*Ctrl*), *Ulk1* siRNA, or *Sec16a* siRNA. Scale bars: 10 µm. **(E–F)** *Ulk2*-ko MEFs transfected with the indicated HA-tagged SEC24 isoform (i.e., A, B, C, or D) and siRNA (i.e., Ctrl, Ulk1, or Sec16a) were fixed and stained with anti-HA antibody, and the number of HA+ puncta per cell was quantified. The data are represented as the mean number (± SEM) of SEC24+ puncta per cell in **E**. Ten HA+ cells per population were scored. $^{\#}P < 0.005$ and $^{*}P < 0.001$ (ANOVA) when compared with the control. Representative immunoblots performed using antibodies against the specified proteins are shown in **F**. **(G–H)** WT and *Ulk1*-ko MEFs were transfected with GFP–SEC16A, fixed, and stained with anti-Sec24C antibody (pseudocolored red) and DAPI (pseudocolored blue). GFP signal was pseudocolored green. Representative merged and single-channel SEC24C (red) pseudocolored images are shown in **G** (lower panels). The mean percentage (± SEM) of $SEC16A^{+}$ puncta in each cell that was costained with SEC24C is shown in **H**. Ten cells were scored for each genotype. Scale bar: 10 µm. $^{*}P < 0.001$ (ANOVA). **(I)** *Ulk1*-ko MEFs stably transduced with the indicated viral vector [i.e., (—), empty vector; WT ULK; or KI ULK1 mutant] were fixed and stained with an antibody against SEC24C. The mean number (±S EM) of $SEC24C^{+}$ puncta per cell are shown. Ten cells per population were scored. $^{*}P < 0.001$ (ANOVA) when compared with empty vector–transduced cells. **(J)** Representative immunoblots of WT MEFs transfected with the indicated siRNAs. The asterisk denotes a nonspecific band migrating below that of ATG14. **(K)** WT and Atg7-ko MEFs were fixed and stained with an antibody against SEC24C. The mean number (± SEM) of $SEC24C^{+}$ puncta per cell is shown. There was no significant difference in the number of SEC24C+ puncta in Atg7-ko MEFs compared to that in WT MEFs (Student's *t*-test). Ten cells per population were scored. **(L)** Representative immunoblot analyses confirm the absence of ATG7 and lipidated LC3 in the *Atg7*-ko MEFs. **(M)** In situ hybridization showing the expression of *Sec24a*, *Sec24b*, *Sec24c*, and *Sec24d* mRNA in the hippocampus of 8-wk-old mice (from the Allen Brain Atlas).

Figure S5, Related to Figure 5.

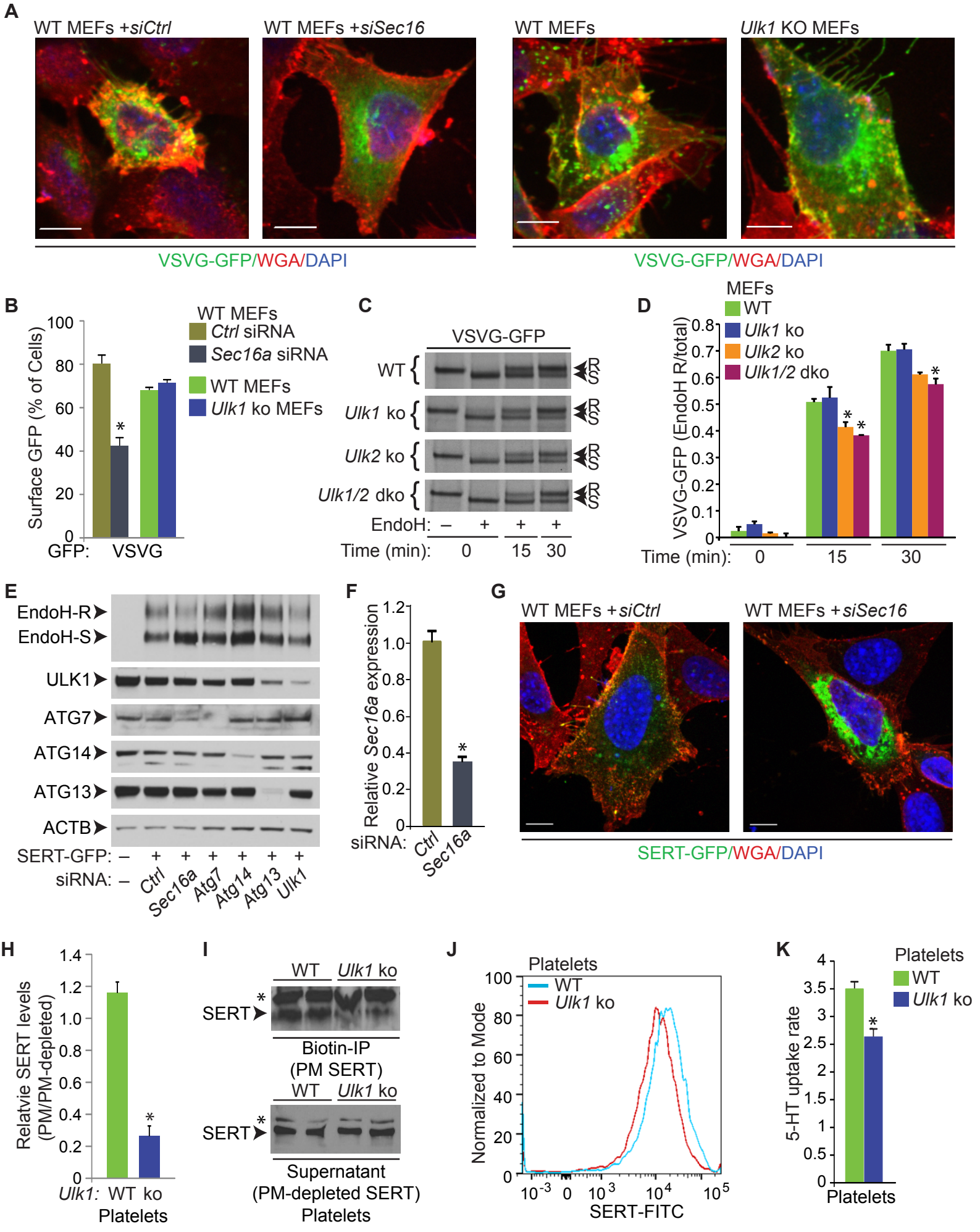

Figure 5S, related to Figure 5. (A) Representative images of WT MEFs cotransfected with VSVG(ts045)-GFP and either control nontargeting siRNA (*siCtrl*) or *siSec16a* siRNA. WT and *Ulk1*-ko MEFs were transfected with VSVG(ts045)-GFP. Cells were stained with Alexa Fluor 647–conjugated wheat germ agglutinin (WGA) (pseudocolored red) to highlight plasma membranes and counterstained with DAPI (pseudocolored blue) to highlight nuclei. GFP signal was pseudocolored green. Scale bar: 10 μm. **(B)** The mean percentages (± SEM) of cells with co-localized WGA and VSVG–GFP. Data were acquired from 3 independent experiments, and more than 100 cells per population were scored in each experiment. **P* < 0.002 (ANOVA) when compared with control (*Ctrl*). **(C)** Representative immunoblots of WT, *Ulk1*-ko, *Ulk2*-ko, and *Ulk1/2*-dko MEFs transfected with VSVG(ts045)-GFP and incubated for 24 h at 41°C. Cells were transferred to a 32°C incubator for the indicated times before whole-cell extracts were prepared. GFP immunoprecipitates (IPs) treated with or without endoglycosidase H (EndoH) were then subjected to immunoblot analysis. R, EndoH-resistant; S, EndoH-sensitive. **(D)** The mean ratios (± SEM) of EndoH-R VSVG to total VSVG from 2 independent IP experiments. **P* < 0.01 (ANOVA) when compared with WT. **(E)** Representative immunoblots of WT MEFs cotransfected with SERT-GFP and the indicated siRNAs. **(F)** RT-qPCR analysis was used to determine the relative mean *Sec16a* mRNA levels (± SEM) in WT MEFs transfected with either *siCtrl* or *Sec16a* siRNA. Data are from 3 independent experiments. **P* < 0.001 (ANOVA) when compared with control. **(G–H)** WT MEFs were cotransfected with SERT-GFP and either *siCtrl* or *Sec16a* siRNA. Cells were stained with Alexa Fluor 647–conjugated WGA (pseudocolored red) to highlight plasma membrane and counterstained with DAPI (pseudocolored blue). GFP signal was pseudocolored green. Representative merged images are shown in **G**. Scale bar: 10 μm. The mean percentages (± SEM) of cells from each population with co-localized WGA and GFP are shown in **H**. Data were acquired from 3 independent experiments, and more than 100 cells per population were scored in each experiment. **P* = 0.003. **(I)** Representative immunoblots of biotin^{+} IPs prepared from platelets isolated from WT or *Ulk1*-ko mice treated with membrane-impermeant NHS-SS-biotin. Asterisks indicate nonspecific bands. **(J)** Platelets from WT and *Ulk1*-ko mice were incubated with anti-SERT antibodies followed by FITC-conjugated secondary antibodies. The samples were analyzed by flow cytometry and gated for single platelets based on forward- and side-scatter profiles. A representative histogram of SERT staining based on 20,000 events is shown. There is a 22% reduction in surface SERT fluorescence intensity in platelets from *Ulk1*-ko mice compared to that in WT mice. **P* = 0.05 (Student's *t*-test). **(K)** The mean rate of 5-HT uptake (± SEM) in platelets from *Ulk1*-ko mice was 25% lower than that in WT littermates. *n* = 3 mice/genotype per assay. **P* < 0.001 (Student's *t*-test).

Figure S6, related to Figure 6.

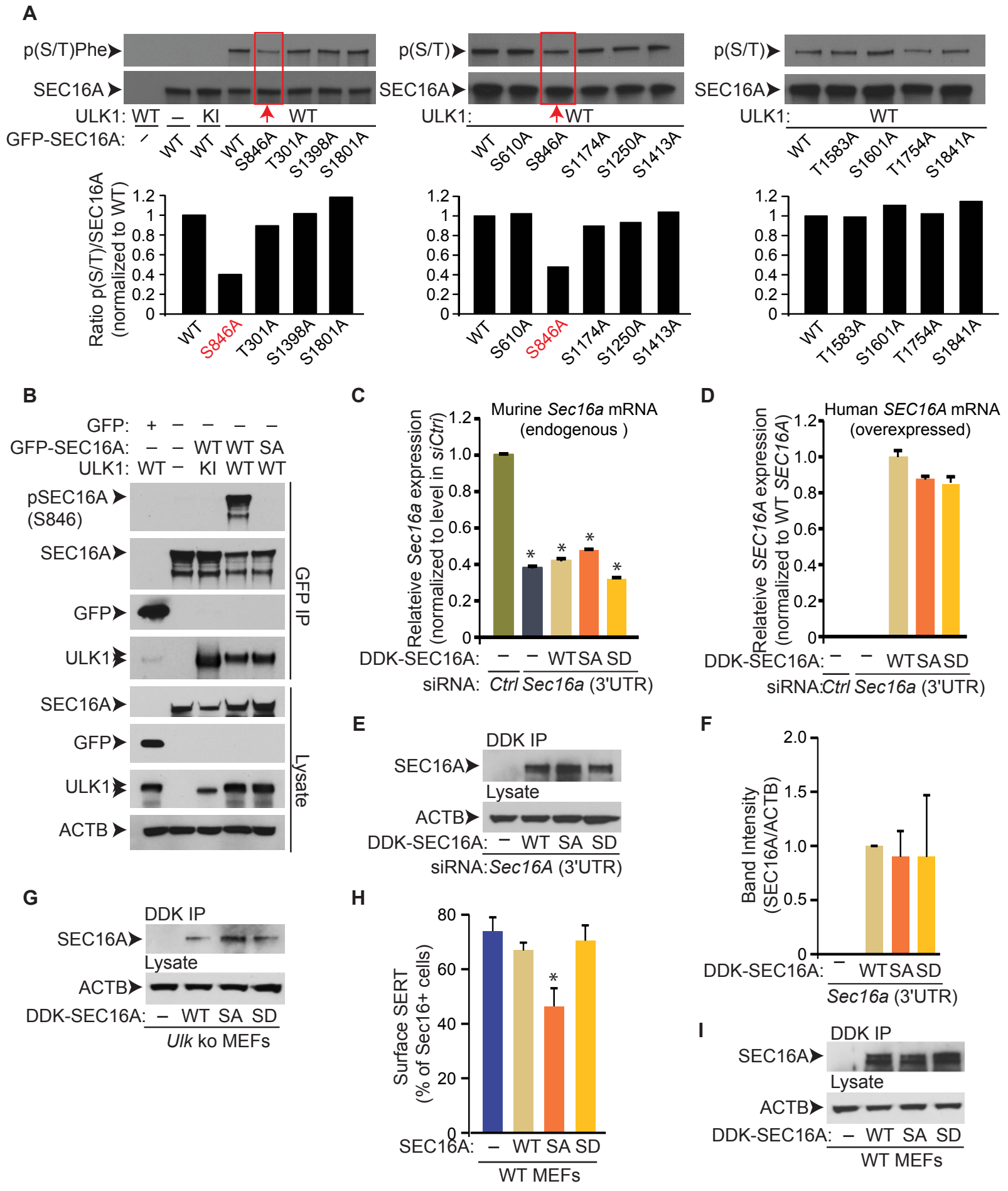

Figure S6, related to Figure 6. (A) GFP^+ immunoprecipitates (IPs) from 293T cells transfected with untagged WT ULK1 or the kinase-inactive (KI) mutant, along with the indicated GFP–SEC16A constructs, were subjected to immunoblot analysis using the anti-p(S/T)Phe antibody to detect phosphorylated SEC16A. The red boxes and arrows highlight the decreased phosphorylation of SEC16A S846A. Several representative immunoblots are shown, along with the corresponding graphs representing the ratio of phosphorylated SEC16A to total SEC16A for each mutant construct. The data from all of the mutants is summarized in Table S1. **(B)** Phospho-specific rabbit polyclonal antibodies were generated against an immunogenic peptide containing pS846 (SEC16A). GFP^+ IPs from 293T cells expressing untagged WT or KI ULK1 and either WT GFP–SEC16A or the S846A (SA) GFP–SEC16A mutant were immunoblotted using this antibody, thereby confirming both the specificity of the antibody and the phosphorylation site. **(C–F)** WT MEFs were transfected with either *Ctrl* or 3′UTR *Sec16a* siRNA and the indicated MYC-DDK–tagged *SEC16A*-expression construct (i.e., WT, SA, or SD). The relative mean levels (± SEM) of endogenous murine *Sec16a* mRNA expression (calibrated to 18S and normalized to levels in MEFs transfected with *Ctrl* siRNA) in each population, based on RT-qPCR analyses, are shown in **C**. Data were acquired from 3 independent experiments. $*P < 0.001$ when compared with *Ctrl* siRNA (ANOVA). The relative mean levels (± SEM) of ectopic human *SEC16A* mRNA expression (calibrated to 18S and normalized to the levels in MEFs transfected with WT SEC16A) in each population, based on RT-qPCR analyses, are shown in **D**. Data were acquired from 3 independent experiments. Anti-MYC antibodies were used to detect ectopic human SEC16A in DDK^+ IPs obtained from each population of cells. Representative immunoblots are shown in **E**. SEC16A band intensities were quantified using ImageJ software and normalized to the band intensity of ACTB in the corresponding samples. Data are represented as means (± SEM, $n = 6$) in **F**. **(G)** *Ulk1* ko MEFs transfected with the indicated MYC-DDK–tagged SEC16A-expression construct (i.e., WT SEC16; S846A, SA; or S846D, SD). Anti-MYC antibodies were used to detect ectopic human SEC16A in DDK^+ IPs obtained from each population of cells. Representative immunoblots are shown. **(H–I)** WT MEFs were cotransfected with SERT-GFP and the indicated MYC-DDK–tagged SEC16A-expression construct [i.e., empty vector (–), WT SEC16A, or SA or SD mutants]. Fixed cells were incubated with Alexa Fluor 647–conjugated WGA before permeabilization and were stained with an anti-DDK antibody. The mean percentages (± SEM) of cells from each population with co-localized WGA and GFP are shown in **H**. Data were acquired from 3 independent experiments, and more than 100 cells per population were scored in each experiment. $*P < 0.05$ (ANOVA) when compared with control (i.e., empty vector). Anti-MYC antibodies were used to detect ectopic human SEC16A in DDK^+ IPs obtained from each population of cells. Representative immunoblots are shown in **I**.

Figure S7, related to Figure 7

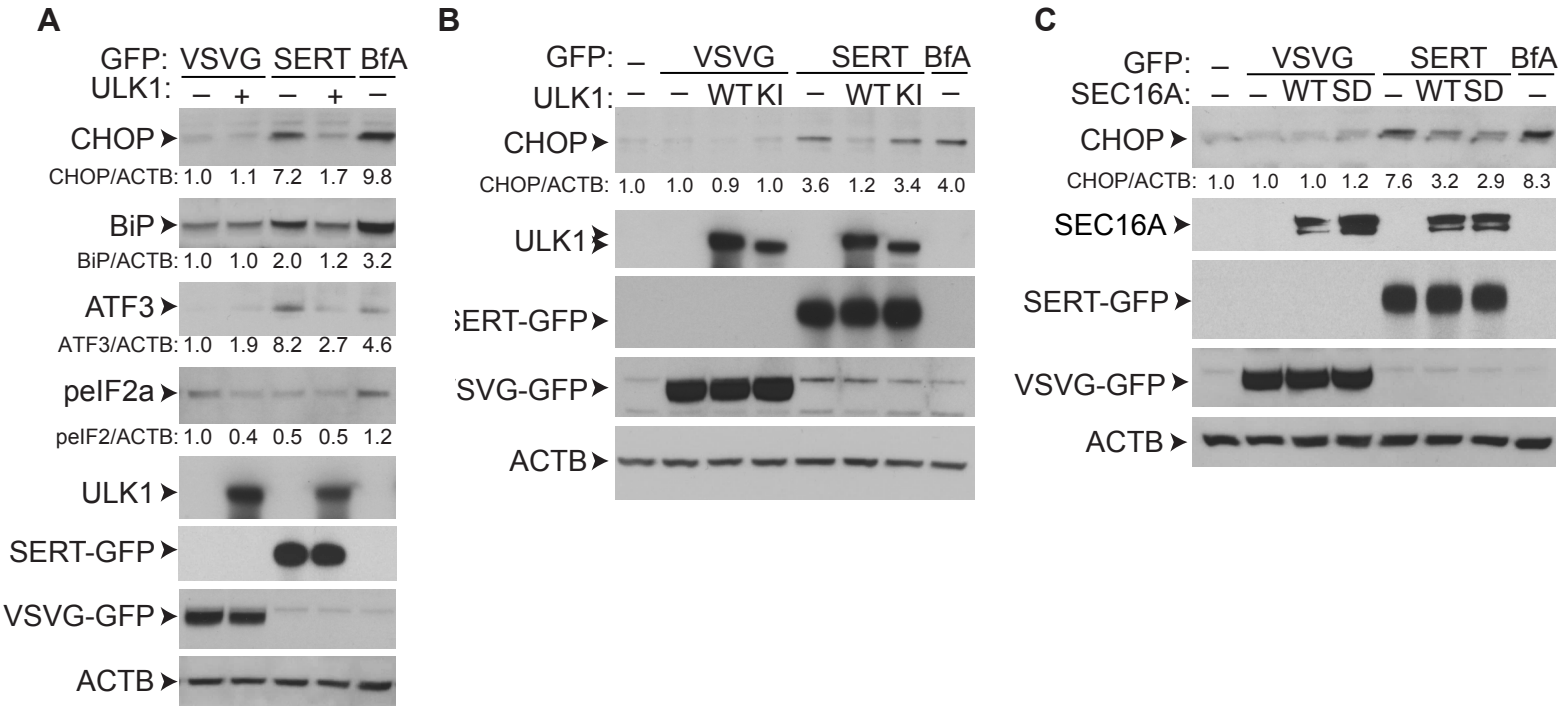

Figure S7, related to Figure 7. (A) Immunoblot analyses of 293T cells transfected with the indicated GFP-tagged construct with or without ULK1. Lysates from 293T cells treated with Brefeldin A at a final concentration of 10 μg/mL for 6 h were included as a positive control. **(B)** Immunoblot analyses of 293T cells cotransfected with the indicated GFP-tagged constructs and WT or KI ULK1. **(C)** Immunoblot analyses of 293T cells cotransfected with the indicated GFP-tagged constructs and WT SEC16A or the S846D mutant (SD). For each immunoblot, the band intensities were quantified using ImageJ software and normalized to the band intensity of ACTB in the corresponding lanes. The SERT-GFP immunoprecipitates were treated with PNGase F to collapse the multiple glycosylated bands into single bands.

Table S1, related to Figure 6. Identification of ULK1 phosphorylation site on SEC16A.

Table S2, related to Figure 6. ULK1 position-specific scoring matrix.

Table S3, related to Figure 6. ULK1 motif scanning in SEC16A.

Table S4, related to Figure 6. SEC16A putative phosphosite conservation.

SUPPLEMENTAL EXPERIMENTAL PROCEDURES

Immunostainings and Histologic Analyses

Mice were transcardially perfused with 4% paraformaldehyde (PFA) and fixed overnight. The brains were then cryoprotected using 30% sucrose in phosphate-buffered saline (PBS) overnight at 4°C and embedded in OCT for cryosectioning. Frozen sections were washed with 0.2% Triton X-100 in tris-buffered saline (TBST) and incubated in the blocking solution (5% normal goat serum or normal donkey serum in TBST) for 1 h at room temperature. Sections were incubated with primary antibodies diluted in the blocking solution overnight at 4°C, washed with TBST, and incubated with Alexa Fluor–conjugated secondary antibodies (Invitrogen), diluted at 1:1000 in the blocking solution for 2 h at room temperature. Sections were mounted in ProLong Gold antifade reagent with DAPI (Invitrogen). Primary antibodies against the following targets were used: NeuN (Synaptic System, 1:500), NeuN (Millipore, 1:1000), Cleaved caspase-3 (Cell Signaling, 1:200), GFAP (Dako, 1:500), Iba1 (Wako, 1:500), P62 (Abnova, 1:500), Ubiquitin (Dako, 1:500), p-S6 (Cell Signaling, 1:400), p-elF2α (Cell Signaling, 1:100), Chop (Santa Cruz, 1:100), BiP (Abcam, 1:500), and ATF6 (Abcam, 1:500), Calbindin (Millipore, 1:500).

For histologic analysis, formalin-fixed brains were processed and embedded in paraffin by using standard methods. Sagittal sections (4-μm) were cut and stained with hematoxylin and eosin (H&E) by staff in the St. Jude Veterinary Pathology Core, and the sections were examined by a pathologist blinded to the experimental groups. Fluoro-Jade C (Millipore, Cat# AG325) staining was carried out on 20-μm frozen sections per the manufacturer's instructions. Quantification of CA1 pyramidal neurons was done with ImageJ software (National Institute of Health, USA). The counts of DAPI in a 500-μm region of CA1 were determined manually. For each animal, the average number of neurons was calculated from at least 5 sections. Cell numbers in the mutants were normalized to their corresponding controls.

Behavioral Analyses

For the limb-clasping test, mice were suspended by pulling their tails. For the rotarod assay, mice were put on a rotating rod, the speed of which gradually increased from 0 to 40 rpm at a rate of 10 rpm/min. The time recorded was when the mouse fell from the rod, and 5 min was used as the cutoff for this analysis. For the gait analysis, the paws of mice were dipped in nontoxic colored ink: fore paws in blue ink and hind paws in red ink. The mice were then allowed to walk through a tunnel placed on top of white paper. The paw prints were then air dried and scanned.

Morphometric Analyses of Electron Micrographs

Mice were deeply anesthetized with CO_2, perfused transcardially with 10 mL phosphate buffer followed by 10 mL 2.5% glutaraldehyde/2% PFA in 0.1 M $CaCO_4$. The brains were removed and fixed in the same fixative and postfixed in 2% osmium tetroxide in 0.1 M sodium cacodylate buffer with 0.3% potassium ferrocyanide for 2 h. Vibratome sections (100-mm) of the brain were cut sagittally and collected in cold PBS, rinsed in phosphate buffer, dehydrated through a series of graded ethanol-to–propylene oxide solutions, infiltrated and embedded in epoxy resin, and polymerized at 70°C overnight. Semithin (0.5-μm) sections were stained with toluidine blue for light microscope examination. Ultrathin (80-nm) sections were cut and imaged using an FEI Tecnai F 20 TEM FEG electron microscope with an AT XR41 camera.

For quantitative analysis of endoplasmic reticulum (ER), all images of neurons in the hippocampal CA1 regions of 2 controls and 2 mutants (8-wk-old) were taken at the same parameters. For each sample, images were randomly obtained from at least 20 neurons. For the quantification of ER number and diameter, the TIFF images were opened with NIS-Elements software (Nikon) and calibrated individually. A 2-μm line was drawn to span as many ER tubules as possible. The number of ER tubules the line crossed was recorded as the ER number. The diameters of the ER tubules covered by the line were also measured individually. To quantify the percentage of ER occupation in the cytosol, the same sets of images were opened in the ImageJ software and calibrated accordingly. Then a 25-μm^2 area was drawn in the cytosol where the ER tubules were the most abundant. The ER tubules in each image were selected and masked manually. The total area of ER in the defined cytosolic region was then measured and recorded. Ten cells from each sample were analyzed.

Plasmid Constructs

The pmGFP-SEC16A (Addgene, Cat# 15775) and pmGFP-SEC16B vectors (Addgene, Cat# 15776) have been previously described (Bhattacharyya and Glick, 2007). SERT–GFP (Origene Technologies, Rockville, MD, Cat# RG210187) and VSVG (ts045)–GFP vectors (Addgene, Cat# 11912) were used in the ER-to-Golgi trafficking assay (Presley et al., 1997). The pCMV6-

MYC-DDK–human SEC16A plasmid (Cat# RC223625), pCMV6-MYC-DDK–human ULK1 (Cat# RC215643), and pCMV6-MYC-DDK-human ULK2 (Cat# RC206010) were purchased from OriGene Technologies. FLAG-tagged ULK1 and deletion constructs in the pME18S vector (a generous gift from Dr. Toshifumi Tomoda, Beckman Research Institute of City of Hope, Duarte, CA) were previously described (Joo et al., 2011; Yan et al., 1998). The FLAG-tagged ULK2 construct in the PCSII vector was a generous gift from Dr. Do-Hyung Kim (University of Minnesota, Twin Cities, MN). Plasmid vectors, $pCS2^{+}$, containing *SEC24A*, *SEC24B*, *SEC24C*, and *SEC24D* open-reading frames, with a 3× HA tag at the N terminus, were described previously (Kim et al., 2007). The Ulk1 and Ulk1 kinase–inactive (KI) (K46A) mutant, as described previously (Joo et al., 2011), were subcloned into the 5′– or 3′–end of EcoR1–restriction enzyme sites of the MSCV-IGFP-MII (generously provided by Dr. Terrence Geiger, St. Jude) and pcDNA3.1 vectors for retrovirus generation and transient transfection, respectively. Human SEC16A phosphorylation-site mutants were introduced into the pmGFP–SEC16A and pCMV6–entry-(MYC-DDK–tagged) human SEC16A vectors by using mutagenic oligonucleotides (see Table below).

Oligonucleotides used to generate SEC16A phosphorylation–site mutants

Mutation sites	**Mutagenic primers**
SEC16A-T301A	Forward: 5′–GACAAGTGCAAATAGT**GCT**TTCGAACCGGTAAAATCTCAC–3′ Reverse: 5′–GATTTTGCCTGAA**TGC**ACTTTCAGGATCAG–3′
SEC16A-S526A	Forward: 5′– GTCATCCAGCTAT**GCC**AGCAGAAGCCACGG –3′ Reverse: 5′– CCGTGGCTTCTGCT**GGC**ATAGCTGGATGAC –3′
SEC16A-T545A	Forward: 5′– GGCCCCAGGAGCTGGTTGGC**GCA**TTCATTCAGCAAGAAGTTGG–3′ Reverse: 5′– CCAACTTCTTGCTGAATGAA**TGC**GCCAACCAGCTCCTGGGGCC –3′
SEC16A-S561A	Forward: 5′– CGAGGATGAAGCTTCAGGT**GCT**TTTTTTAAGC –3′ Reverse: 5′– GCTTAAAAAA**AGC**ACCTGAAGCTTCATCCTCG –3′
SEC16A-S610A	Forward: 5′–GACAAGTGCAAATAGT**GCT**TTCGAACCGGTAAAATCTCAC–3′ Reverse: 5′–GTGAGATTTTACCGGTTCGAA**AGC**ACTATTTGCACTTGTC–3′
SEC16A-S846A	Forward: 5′–GGCTCAGCCCATTAACTTT**GCT**GTGTCCTTATCGAACTC–3′ Reverse: 5′–GAGTTCGATAAGGACAC**AGC**AAAGTTAATGGGCTGAGCC–3′
SEC16A-T997A	Forward: 5′– CGGAGCCCTAGACTTT**GCC**TTAAGCAGGAC –3′ Reverse: 5′– GTCCTGCTTAA**GGC**AAAGTCTAGGGCTCCG –3′
SEC16A-S1079A	Forward: 5′–CAAAGCCATGTTT**GCG**GAGCTGTCAAATCC–3′ Reverse: 5′–GGATTTGACAGCTC**CGC**AAACATGGCTTTG–3′
SEC16A-S1174A	Forward: 5′–GCCTACCAGCCTCAGTAC**GCT**TTGCCGTACCCACCGGAG–3′ Reverse: 5′- CTCCGGTGGGTACGGCAA**AGC**GTACTGAGGCTGGTAGGC –3′
SEC16A-S1193A	Forward: 5′–CCAGGATGTCTAC**GCC**CTCTATGAGCCTCG–3′ Reverse: 5′–CGAGGCTCATAGAG**GGC**GTAGACATCCTGG–3′
SEC16A-S1244A	Forward: 5′–CCTGAAGGATACTAT**GCT**TCCAAAAGTGG–3′ Reverse: 5′–CCACTTTTGGA**AGC**ATAGTATCCTTCAGG–3′
SEC16A-S1250A	Forward: 5′–GTTCCAAAAGTGGATGG**GCC**AGTCAGAGCGATTACTATGC–3′ Reverse: 5′–GCATAGTAATCGCTCTGACT**GGC**CCATCCACTTTTGGAAC–3′
SEC16A-S1261A	Forward: 5′–CTATGCAAGCTATTAC**GCC**AGCCAGTACG–3′ Reverse: 5′–CGTACTGGCT**GGC**GTAATAGCTTGCATAG–3′
SEC16A-S1278A	Forward: 5′–GATCGTTACCACTAC**GCT**GCTAGAGTCAGG-3′ Reverse: 5′-CCTGACTCTAGC**AGC**GTAGTGGTAACGATC–3′
SEC16A-T1325A	Forward: 5′–CGATCCTCGCTTC**GCG**GGGAGTTTTGACG–3′ Reverse: 5′–CGTCAAAACTCCC**CGC**GAAGCGAGGATCG–3′
SEC16A-S1327A	Forward: 5′– CGATCCTCGCTTCACGGGG**GCT**TTTGACGATGACCCCGATCC –3′ Reverse: 5′– GGATCGGGGTCATCGTCAAA**AGC**CCCCGTGAAGCGAGGATCG –3′
SEC16A-S1398A	Forward: 5′–CGAGGCCCCGCTTCCTCCAGGC**GCC**TTTCACGGCGATTTGCC–3′ Reverse: 5′–GGCAAAATCGCCGTGAAA**GGC**GCCTGGAGGAAGCGGGGCCTCG–3′
SEC16A-S1413A	Forward: 5′–GCACCTACCGCAGCAATTTC**GCC**AGTGGCCCCGGCTTCCC–3′ Reverse: 5′–GGGAAGCCGGGGCCACT**GGC**GAAATTGCTGCGGTAGGTGC–3′
SEC16A-S1446A	Forward: 5′– CCAACTTCTCCTGAAAAATTT**GCA**GTGCCTCATGTCTGTGCCAGG –3′ Reverse: 5′– CCTGGCACAGACATGAGGCA**CTGC**AAATTTTTCAGGAGAAGTTGG –3′
SEC16A-T1583A	Forward: 5′–GCAAACCTGATTGATTTC**GCG**AATGAGGCAGTGGAGCAGG-3′ Reverse: 5′-CCTGCTCCACTGCCTCATT**CGC**GAAATCAATCAGGTTTGC-3′
SEC16A-S1601A	Forward: 5′–GTCTGGTGAGGCCCAGCTC**GCT**TTCCTCACTGGTGGTCCG–3′ Reverse: 5′-CGGACCACCAGTGAGGAA**AGC**GAGCTGGGCCTCACCAGAC-3′
SEC16A-	Forward: 5′-CAGGCGGGATTTGGTGTTTAC**GCG**AAGAAAACTACAAAGC-3′

T1754A	Reverse: 5′-GCTTTGTAGTTTTCTT**CGC**GTAAACACCAAATCCCGCCTG-3′
SEC16A-S1801A	Forward: 5′-CGAGACCTGCCCCCTGCCT**GCT**TTCCAGGTGTTTAAGTTCATC-3’ Reverse: 5’-GATGAACTTAAACACCTGGAA**AGC**AGGCAGGGGGCAGGTCTCG-3’
SEC16A-S1810A	Forward: 5′- CGAGACCTGCCCCCTGCCT**GCT**TTCCAGGTGTTTAAGTTCATC -3’ Reverse: 5’- GATGAACTTAAACACCTGGAA**AGC**AGGCAGGGGGCAGGTCTCG -3’
SEC16A-S1841A	Forward: 5′-CCTGACGCAGCCGCACCTGTAT**GCC**CCGGTGTTGATCAGCCAGC-3′ Reverse: 5′-GCTGGCTGATCAACACCGG**GGC**ATACAGGTGCGGCTGCGTCAGG-3′
SEC16A-S2183A	Forward: 5′-CCGTGAACATGTAC**GCT**AGAAGAGCAGCAG-3′ Reverse: 5′-CTGCTGCTCTTCT**AGC**GTACATGTTCACGG-3′

Generation of Murine Embryonic Fibroblasts, Cell Culture, Transfection, Gene Silencing, and Drug Treatment

Ulk1-ko, *Ulk2*-ko, and *Ulk1/2*-dko murine embryonic fibroblasts (MEFs) were prepared from the E12.5 embryos of $Ulk1^{+/-}$; $Ulk2^{+/-}$ × $Ulk1^{+/-}$;$Ulk2^{+/-}$ crosses. Embryos were collected, washed twice with PBS, incubated in trypsin, and then separated into single-cell suspensions. Cells were expanded in DMEM (Invitrogen) supplemented with 10% fetal bovine serum (FBS) (Hyclone), MEM nonessential amino acids (NEAA; Life Technologies), *L*-glutamine (Life Technologies), β-mercaptoethanol (Life Technologies), and gentamycin (Life Technologies). These primary MEFs were then immortalized using FuGENE™ 6 (Roche) to transfect the cells with 1 μg of an expression vector expressing SV40, as described previously (Joo et al., 2011).

After transfection, cells were maintained in normal growth media. $Atg7^{-/-}$ MEFs and stably transduced MEFs were generated as described previously (Joo et al., 2011). Briefly, MSCV-IGFP-MII containing no cDNA (empty vector), WT ULK1, or mutant ULK1, and helper vector (generously provided by Dr. Terrence Geiger) were cotransfected into 293T cells by using FuGENE 6. Transfected cells were then incubated in DMEM with 10% FBS for 48 h. Supernatant was collected twice daily and used to infect GP+E86 retroviral–producer cells in the presence of Polybrene (8 μg/mL). Transduced GP+E86 cells were FACS-sorted by the presence of GFP, and cell-free supernatant was used to transduce $Ulk1^{-/-}$ MEFs. MEFs and 293T cells were grown in DMEM supplemented with 10% FBS, penicillin/streptomycin (Invitrogen), and Glutamax (Invitrogen) at 37°C (5% CO_2). The cells were transfected with FuGENE 6 according to the manufacturer's protocol for transient overexpression of cDNA constructs.

Knockdown experiments in MEFs were performed using Lipofectamine RNAi Max (Life Technologies) per the manufacturer's protocol and with the following siRNA constructs obtained from Dharmacon: pooled nontargeting siRNA (D-001810-10-05), SMARTpool: ON-TARGETplus *Ulk1* siRNA (L-040155-00-0005); SMARTpool: ON-TARGETplus *Sec16a* siRNA (L058170-02-0005); ON-TARGETplus *Sec16a* siRNA Targeted Region: 3'UTR (J-058170-11-0005); SMARTpool: ON-TARGETplus *Sec24a* siRNA (L-056263-01-0005); SMARTpool: ON-TARGETplus *Sec24b* siRNA (L-048898-01-0005); SMARTpool: ON-TARGETplus *Sec24c* siRNA (L-059052-01-0005); SMARTpool: ON-TARGETplus *Sec24d* siRNA (L-065430-01-0005); SMARTpool: ON-TARGETplus *Atg7* siRNA (L-049953-00-0005);SMARTpool: ON-TARGETplus *Atg13* siRNA (L-053540-01-0005); and SMARTpool: ON-TARGETplus *Atg14* siRNA (L-172696-00-0005). Knockdown was confirmed by RT-qPCR (TaqMan) analyses, immunoblot analyses, or both. To chemically induce ER stress, 293T cells were treated with Brefeldin A (Sigma Aldrich) and dissolved in DMSO (final concentration, 10 μg/mL) for 6 h. Cells were then lysed and analyzed by immunoblotting.

Immunoblot Analyses and Antibodies

Whole hippocampi or MEF cells were lysed in Triton-based cell lysis buffer. Proteins in cleared lysates were electrophoretically separated on 4% to 12% bis-Tris gels (Life Technologies). Proteins were then transferred to either a nitrocellulose or a PVDF membrane.

After incubation with a 5% skim milk block, blots were probed with antibodies directed against the following targets: P62 (Sigma Aldrich, Cat# P0067), LC3 (MBL, Cat# PM036) ULK1 (Sigma Aldrich, Cat# A7481), p-ULK1 (S555) (Cell Signaling, Cat# 5869), p-(Ser/Thr) Phe (Cell Signaling, Cat# 9631), SEC16A (Novus, Cat# NB100-1799), SEC16A pS846 (custom polyclonal antibody from Rockland), ATG7 (Cell Signaling, Cat# 2631), ATG13 (Sigma Aldrich, Cat# SAB4200100), p-ATG13 (S318) (Rockland, Cat# 600-401-C49), ATG14 (MBL, Cat# PD026), CDC37 (Santa Cruz Biotechnology, Cat# sc-13129), SERT (Millipore, Cat# PC177L), ATF3 (NOVUS, Cat# NBP1-02935), p-elf2α (Cell Signaling, Cat# 3597), CHOP and BIP (a generous gift from Dr. Linda Hendershot, St. Jude), GFP (Abcam, Cat# ab6556), FLAG (Sigma Aldrich, Cat# F1804), HA (Cell Signaling, Cat# 3724), Myc (Cell Signaling, Cat# 2276), DDK (OriGene, Cat# TA50011-100), ACTB (Santa Cruz Biotechnology, Cat# I-19), and GAPDH (Sigma Aldrich, Cat# G9545). Membranes were then incubated with horseradish peroxidase–conjugated secondary antibodies, and bands were detected using chemiluminescence-detection kits (Amersham).

Proteomics

The mass spectrometric (MS) analysis was performed per an optimized platform, as previously reported (Xu et al., 2009). ULK1-interacting proteins were visualized by performing silver staining (Life Technologies) or SYPRO Ruby protein gel staining (Sigma Aldrich) according to the manufacturer's protocol. Proteins in gel bands were reduced by adding dithiothreitol (DTT) and then alkylated by adding iodoacetamide. The gel bands were washed, dried in a speed vacuum, and rehydrated with a trypsin-containing buffer for overnight proteolysis. The digested peptides were extracted, dried, reconstituted, and loaded onto a capillary reverse-phase C18 column by an HPLC system (Waters ACQUITY UPLC). Peptides were eluted in a gradient, ionized by electrospray ionization, and detected by an in-line mass spectrometer (Thermo scientific LTQ Orbitrap Elite). MS spectra were collected, and the top 20 abundant ions were sequentially isolated for MS/MS analysis. This process was cycled over the entire liquid chromatography gradient. The acquired MS/MS spectra were used to search protein databases to obtain possible peptide matches. All matched MS/MS spectra were filtered by mass accuracy and matching scores to reduce the protein false-discovery rate to less than 1%.

Quantitative Real-Time PCR

Total RNA of adult hippocampi was extracted with RNeasy Mini Kit (Qiagen) according to the manufacturer's instructions. Total RNA was isolated from cells by using TRIzol Reagent (Life Technologies). The reverse-transcription reaction was carried out using the SuperScript III first-strand synthesis kit (Life Technologies) per the manufacturer's instructions. TaqMan gene-expression assays containing FAM-labeled primer/probe sets specific for *Ulk1* (Mm-00437238_m1), *Ulk2* (Mm-00497023_m1), *Sec16a* (Mm00462283_m1), *Sec24a* (Mm00613960_m1), *Sec24b* (Mm01313235_m1), *Sec24c* (Mm00655499_m1), *Sec24d* (Mm00660744_m1), and *18S* were obtained from Applied Biosystems. The real-time PCR reactions were performed in a total reaction volume of 25 µL by using FastStart TaqMan Probe Master (Roche) reagent, and results were analyzed using the ABI 7900 real-time PCR-detection system (Applied Biosystems). Relative expression was normalized to *18S* RNA and calibrated to the respective controls.

Immunofluorescence Microscopy

To assess SEC24C puncta quantity and ULK1 distribution, MEFs were incubated in complete growth media, fixed in 4% PFA, permeabilized with digitonin (100 µg/mL in PBS), blocked in 1% BSA, and then labeled with one of the following antibodies: anti-ULK1, anti-SEC24C (Abcam, ab122635), anti-HA or anti-FLAG. Cells were then treated with secondary antibodies conjugated to Alexa-555 or Alexa-647 (Invitrogen). To assess endogenous SEC16A distribution, MEFs were fixed in cold methanol for 15 min; slowly brought to room temperature in PBS; and blocked in PBS, 4% BSA, and 0.1% Triton X-100. MEFs were then labeled with anti-SEC16A antibody (Bethyl Laboratories, Cat# KIAA0310), followed by Cy3-conjugated secondary antibody (Jackson Immunoresearch, Cat# 711-165-152). To evaluate VSVG–GFP and SERT–GFP trafficking, MEFs were fixed and prestained with wheat germ agglutinin and Alexa Fluor 647 conjugate (Life Technologies, Cat# W32466) and then permeabilized with Triton X-100 (100 µg/mL in PBS) if additional staining with anti-FLAG antibody was needed.

To quantify SEC24C and GFP-SEC16A puncta, MEFs were imaged using a spinning-disc confocal Zeiss AxioObserver operated by Marianas system (Intelligent Imaging Innovations, Denver CO) with a 63× oil objective, and the number of puncta was analyzed using SlideBook 5.5 software (Intelligent Imaging Innovations, Denver CO). To quantify endogenous SEC16A puncta, MEFs were imaged using a swept-field confocal microscope (Nikon Ti-E) equipped with a Roper CoolSNAP HQ2 CCD camera using a Nikon 60×, 1.4 numerical aperture plan apochromat oil objective lens. Acquisition parameters were controlled by NIS-Elements software, and image analysis was conducted using Metamorph software. Confocal microscopy of ULK1 and GFP–SEC16A colocalization was performed on a Nikon TE2000E2 microscope equipped with a Nikon C2 confocal microscope using 488-nm, 561-nm, and 638-nm DPSS lasers for excitation. Images were acquired using a Nikon 60× 1.45 NA objective and analyzed using the NIS-Elements software. The following filters were used: 515/60, 605/75, and 675/50. VSVG-GFP– and SERT-GFP–transfected MEFs were imaged using a spinning-disc confocal Zeiss AxioObserver operated by Marianas system (Intelligent Imaging Innovations, Denver CO) with a 63× oil objective.

To quantify nuclear localization of CHOP, MEFs were grown in normal growth medium, transiently transfected with VSVG (ts045)–GFP or SERT–GFP, and immunostained with anti-CHOP antibody (Santa Cruz, Cat# sc-575). At least 30 images were acquired, as described above for each condition. The percentage of cells with nuclear CHOP was obtained from 3 independent experiments. As a positive control, the MEFs were treated with Brefeldin A (10 µg/mL) for 6 h, after which 100% nuclear localization of CHOP was observed.

Immunofluorescence Microscopy in C. elegans

C. elegans gonads were dissected on poly-L-lysine–coated slides, frozen in liquid nitrogen, and methanol-fixed at –20°C (Audhya et al., 2005). Tissues were immunostained using a polyclonal rabbit antibody directed against *C. elegans* SEC16 (Witte et al., 2011) and subsequently labeled with a Cy3-conjugated anti-rabbit secondary antibody. Proximal oocytes were examined on a Nikon Ti-E swept-field confocal microscope, with a Roper CoolSNAP HQ2 CCD camera and using a Nikon 60× 1.4 numerical aperture plan apochromat oil objective lens. Acquisition was controlled using NIS-Elements software, and image analysis was performed using Imaris Bitplane software. Thirty z-sections at 0.2-µm steps were acquired. The number and fluorescence intensities of SEC16 puncta were quantified using the Spots module of Imaris Bitplane in at least 10 animals for each condition. Puncta fluorescence was classified as low-, medium-, or high-intensity thresholds, and the percentage of puncta in each category was compared between N2 control and *unc-51*–mutant animals. Immunostaining of rabbit anti–MOD-5 antibody (Jafari et al., 2011) and rabbit anti–5-HT antibody (purchased from Dr. H.W.M. Steinbusch, Maastricht University, Masstricht, The Netherlands) was performed with whole-mount WT worms and *mod-5(n314)* and *unc-51*(e369) mutants, as described previously (Jafari et al., 2011; Sze et al., 2000).

C. elegans Extract Preparation and Immunoblotting

Adult *C. elegans* hermaphroditic worms were grown synchronously in liquid culture, and whole-worm lysates were generated as previously described (Witte et al., 2011). Whole-worm extract was fractionated on a Superose 6 gel-filtration chromatography column. Fractions were probed with antibodies against SEC13 and SEC23. Intensities of bands in each fraction were normalized and averaged across 3 blots to generate the protein-distribution profiles.

Endoglycosidase H Assay

The Endo H assay for monitoring ER-to-Golgi trafficking of VSVG was performed as previously reported (Petrova et al., 2008; Shen and Hendershot, 2005). Briefly, VSVG(ts045)-GFP–transfected MEFs in 100-mm tissue culture dishes were washed once with PBS before 5 mL Met-/Cys-labeling DMEM media (17-204-CI, Corning Cellgro, Manassas, VA, Cat# 17-204-CI) supplied with 10% dialyzed FBS (Gibco, Life Technologies, Cat# 26400-036) was added and incubated for 30 min in a 41°C incubator. Then, 500 µCi ^{35}S-Met^{+}/Cys^{+} was added, and the MEFs were incubated in a 32°C incubator for 15 or 30 min. Labeled cells were lysed in NP40 lysis buffer (50 mM Tris-HCL, PH 7.5, 150 mM NaCl, 0.5% sodium deoxycholate, 0.5% NP-40, and 2% $NaNH_3$), and the supernatant was used for GFP immunoprecipitation. Immunopurified proteins were treated with Endo H enzyme (New England BioLabs, Cat# P0702L) for 1 h per the manufacturer's instructions. Endo H–digested samples were electrophoretically separated in 4% to 12% Bis-Tris gels, transferred to filter paper, and then exposed to Biomax MR film (Carestream, Rochester, NY, Cat# 870 1302). For monitoring ER-to-Golgi trafficking of SERT, extracts prepared from SERT-GFP–transfected MEFs were used for GFP immunoprecipitation. Immunopurified proteins were incubated in the presence or absence of Endo H enzyme or peptide-N-glycosidase F (PNGase) enzyme (New England Biolabs, Cat# P0704) for 1 h, eluted from the beads in SDS sample buffer with β-mercaptoethanol, and separated by SDS-PAGE. SERT was detected by immunoblot analysis. Glycosylated proteins such as SERT and VSVG are Endo H–sensitive (Endo H–S) while in the ER, and become Endo H–resistant (Endo H–R) after ER-to-Golgi trafficking. PNGase treatment results in deglycosylated proteins.

Cell-Surface Biotinylation

The levels of SERT expression in MEFs or platelet PMs were compared using the membrane-impermeant biotinylation reagent, NHS-SS-biotin (Pierce, Inc., Rockford, IL), as described previously (Brenner et al., 2007; Ziu et al., 2012). Briefly, platelet or MEF pellets were washed twice with ice-cold PBSCM solution (PBS containing 0.1 mmol/L $CaCl_2$ and 1 mmol/L $MgCl_2$), incubated with NHS-SS-biotin (1.5 mg/mL) on ice with very gentle shaking for 20 min, rinsed briefly, incubated with PBSCM containing 100 mmol/L glycine on ice for 20 min, and lysed with 1% SDS–1% Triton X-100. Biotinylated PM proteins were recovered from the cell lysates by using streptavidin-agarose beads (Pierce, Inc.). After washing the beads with high-salt, low-salt, and 50 mmol/L Tris-HCl (pH 7.5), the biotinylated proteins were treated with either Endo H enzyme or PNGase F enzyme (New England Biolabs, Cat# P0704) for 1 h, eluted from the beads in SDS sample buffer with β-mercaptoethanol, and separated by SDS-PAGE. SERT was detected by immunoblot analysis.

Blood Sampling and Platelet Preparation

Blood samples were drawn from the retro-orbital plexus of mice by using capillary tubes. Samples of platelets and plasma were prepared from the whole blood as described previously (Brenner et al., 2007; Ziu et al., 2012). Briefly, peripheral blood samples

were mixed with Tyrode HEPES buffer (134 mmol/L NaCl, 0.34 mmol/L Na_2HPO_4, 2.9 mmol/L KCl, 12 mmol/L $NaHCO_3$, 20 mmol/L HEPES, 5 mmol/L glucose, 1 mmol/L $MgCl_2$, pH 7.3) and centrifuged at 200 ×g for 7.5 min at 20°C-25°C. The supernatants consisting of platelet-rich plasma were transferred to fresh Eppendorf tubes containing Tyrode HEPES (1:0.5 volume). Samples were then centrifuged at 200 ×g for 7.5 min at 20°C-25°C. The supernatants were centrifuged again at 1000 ×g for 5 min, and the platelet pellets were resuspended in the appropriate buffer for biochemical studies.

Flow Cytometry

The level of SERT on the surface of platelets was determined by flow cytometry using an antibody generated by Proteintech Group, Inc. (Chicago, IL) against a synthetic peptide corresponding to the second extracellular loop of SERT, which is not affected by posttranslational modifications of SERT (e.g., glycosylation and disulfide-bond formation). Platelets were first stained with anti-SERT antibody and FITC-conjugated anti–rabbit IgG. Then they were processed as described previously (Brenner et al., 2007; Li et al., 2014; Ziu et al., 2012). The samples were gated for single platelets based on forward- and side-scatter profiles, and 20,000 events were collected. These studies were done by staff at the University of Arkansas for Medical Sciences Flow Cytometry Core Facility.

Platelet 5-HT–Uptake Assay

The platelet 5-HT–uptake assay was performed as previously described (Brenner et al., 2007; Ziu et al., 2012). Briefly, platelet pellets were washed with PBSCM, resuspended in PBSCM with 14.6 nmol/L ^{3}H-5HT, and then incubated at room temperature for 10 min. Platelets were collected by rapid filtration through Whatman GF/B filters, which were washed twice with 5 mL ice-cold PBS and placed in scintillation vials containing 5 mL scintillation cocktail for immediate quantification of ^{3}H.

Background accumulation of ^{3}H-5HT, which occurred independently of SERT, was measured in the same experiment in which platelets were treated with the high-affinity cocaine analog 0.1 μmol/L 2β-carbomethoxy-3-tropane (β-CIT) (Chemical Synthesis Service, NIMH, Bethesda, MD) and subtracted from each experimental value. In parallel, the protein concentration for 0.2×10^6 platelets (i.e., 0.015 mg cellular protein) was determined using the Micro BCA Protein Assay Kit (Pierce, Inc). The 5-HT–uptake rates of transporters were calculated as the means and standard deviations from 3 independent experiments.

Identification of Putative SEC16A Phosphosites Modified by the ULK1 Kinase

We estimated putative SEC16A Ser/Thr residues phosphorylated by ULK1 by two methods: (i) ULK1 kinase binding motif, and (ii) the conservation of putative SEC16A phosphosites in different organisms ranging from yeast to human.

The ULK1 kinase binding motif was defined by the ULK1 position-specific scoring matrix (Gribskov et al., 1987) from the Reuben Shaw group's peptide array data (Egan et al., 2015) and then searched in the SEC16A protein sequence (NP_055681.1). An odds ratio method was used to score each putative phosphorylation site (Henikoff and Henikoff, 1996):

$$score(i) = \sum_{i=1}^{n} -\log(\frac{P_m(i)}{P_{background}(i)})$$

Based on the ULK1 scoring matrix m with n positions, each position i was examined whether the sequence is more probable to be part of the ULK1 binding site $P_m(i)$ compared to its background $P_{background}(i)$ amino acid content. To ensure the score represent positions with high information content, positions i of {-3, 0, 1, 2} were used in the scoring.

For each putative phosphorylation site, the conservation for Ser/Thr residues was assessed. Vertebrate ortholog for SEC16A was downloaded from the NCBI homology database (Wheeler et al., 2005): *Homo sapiens* (NP_055681.1), *Pan trogliodytes* (XP_001171528.2), *Macaca mulatta* (XP_001117942.2), *Canis lupus* (XP_005625160.1), *Bos taurus* (XP_002691705.1), *Mus musculus* (NP_694765.2), *Rattus norvegicus* (NP_001263346.1), *Gallus gallus* (XP_415419.4), *Xenopus tropicalis* (XP_004916692.1), and *Danio rerio* (XP_695457.6). A representative set of non-vertebrate homologs for SEC16A were also downloaded from NCBI sequence database: *Saccharomyces cerevisiae* (NP_015240.1), *Drosohpila melanogaster* (NP_572812.3), and *Caenohabditis elegans* (NP_499022.1). The multiple sequence alignment algorithm MUSCLE (Edgar, 2004) was run from the EMBL-EBI web server (McWilliam et al., 2013) under default conditions. Based on each sequence's alignment to the human SEC16A, an algorithm was devised to calculate the percentage of conserved Ser or Thr residues at each putative phosphosite.

SUPPLEMENTAL REFERENCES

Audhya, A., Hyndman, F., McLeod, I.X., Maddox, A.S., Yates, J.R., 3rd, Desai, A., and Oegema, K. (2005). A complex containing the Sm protein CAR-1 and the RNA helicase CGH-1 is required for embryonic cytokinesis in Caenorhabditis elegans. J. Cell Biol. *171*, 267-279.

Bhattacharyya, D., and Glick, B.S. (2007). Two mammalian Sec16 homologues have nonredundant functions in endoplasmic reticulum (ER) export and transitional ER organization. Mol. Biol. Cell *18*, 839-849.

Brenner, B., Harney, J.T., Ahmed, B.A., Jeffus, B.C., Unal, R., Mehta, J.L., and Kilic, F. (2007). Plasma serotonin levels and the platelet serotonin transporter. J. Neurochem. *102*, 206-215.

Edgar, R.C. (2004). MUSCLE: multiple sequence alignment with high accuracy and high throughput. Nucleic Acids Res. *32*, 1792-1797.

Egan, D.F., Chun, M.G., Vamos, M., Zou, H., Rong, J., Miller, C.J., Lou, H.J., Raveendra-Panickar, D., Yang, C.C., Sheffler, D.J., *et al.* (2015). Small Molecule Inhibition of the Autophagy Kinase ULK1 and Identification of ULK1 Substrates. Mol. Cell *59*, 285-297.

Gribskov, M., McLachlan, A.D., and Eisenberg, D. (1987). Profile analysis: detection of distantly related proteins. Proc. Natl. Acad. Sci. U. S. A. *84*, 4355-4358.

Henikoff, J.G., and Henikoff, S. (1996). Using substitution probabilities to improve position-specific scoring matrices. Comput. Appl. Biosci. *12*, 135-143.

Jafari, G., Xie, Y., Kullyev, A., Liang, B., and Sze, J.Y. (2011). Regulation of extrasynaptic 5-HT by serotonin reuptake transporter function in 5-HT-absorbing neurons underscores adaptation behavior in Caenorhabditis elegans. J. Neurosci. *31*, 8948-8957.

Joo, J.H., Dorsey, F.C., Joshi, A., Hennessy-Walters, K.M., Rose, K.L., McCastlain, K., Zhang, J., Iyengar, R., Jung, C.H., Suen, D.F., *et al.* (2011). Hsp90-Cdc37 chaperone complex regulates Ulk1- and Atg13-mediated mitophagy. Mol. Cell *43*, 572-585.

Kim, J., Kleizen, B., Choy, R., Thinakaran, G., Sisodia, S.S., and Schekman, R.W. (2007). Biogenesis of gamma-secretase early in the secretory pathway. J. Cell Biol. *179*, 951-963.

Li, Y., Hadden, C., Singh, P., Mercado, C.P., Murphy, P., Dajani, N.K., Lowery, C.L., Roberts, D.J., Maroteaux, L., and Kilic, F. (2014). GDM-associated insulin deficiency hinders the dissociation of SERT from ERp44 and down-regulates placental 5-HT uptake. Proc. Natl. Acad. Sci. U. S. A. *111*, E5697-5705.

McWilliam, H., Li, W., Uludag, M., Squizzato, S., Park, Y.M., Buso, N., Cowley, A.P., and Lopez, R. (2013). Analysis Tool Web Services from the EMBL-EBI. Nucleic Acids Res. *41*, W597-600.

Petrova, K., Oyadomari, S., Hendershot, L.M., and Ron, D. (2008). Regulated association of misfolded endoplasmic reticulum lumenal proteins with P58/DNAJc3. EMBO J. *27*, 2862-2872.

Presley, J.F., Cole, N.B., Schroer, T.A., Hirschberg, K., Zaal, K.J., and Lippincott-Schwartz, J. (1997). ER-to-Golgi transport visualized in living cells. Nature *389*, 81-85.

Shen, Y., and Hendershot, L.M. (2005). ERdj3, a stress-inducible endoplasmic reticulum DnaJ homologue, serves as a cofactor for BiP's interactions with unfolded substrates. Mol. Biol. Cell *16*, 40-50.

Sze, J.Y., Victor, M., Loer, C., Shi, Y., and Ruvkun, G. (2000). Food and metabolic signalling defects in a Caenorhabditis elegans serotonin-synthesis mutant. Nature *403*, 560-564.

Wheeler, D.L., Barrett, T., Benson, D.A., Bryant, S.H., Canese, K., Church, D.M., DiCuccio, M., Edgar, R., Federhen, S., Helmberg, W., *et al.* (2005). Database resources of the National Center for Biotechnology Information. Nucleic Acids Res. *33*, D39-45.

Witte, K., Schuh, A.L., Hegermann, J., Sarkeshik, A., Mayers, J.R., Schwarze, K., Yates, J.R., 3rd, Eimer, S., and Audhya, A. (2011). TFG-1 function in protein secretion and oncogenesis. Nat. Cell Biol. *13*, 550-558.

Xu, P., Duong, D.M., and Peng, J. (2009). Systematical optimization of reverse-phase chromatography for shotgun proteomics. J. Proteome Res. *8*, 3944-3950.

Yan, J., Kuroyanagi, H., Kuroiwa, A., Matsuda, Y., Tokumitsu, H., Tomoda, T., Shirasawa, T., and Muramatsu, M. (1998). Identification of mouse ULK1, a novel protein kinase structurally related to C. elegans UNC-51. Biochem. Biophys. Res. Commun. *246*, 222-227.

Ziu, E., Mercado, C.P., Li, Y., Singh, P., Ahmed, B.A., Freyaldenhoven, S., Lensing, S., Ware, J., and Kilic, F. (2012). Down-regulation of the serotonin transporter in hyperreactive platelets counteracts the pro-thrombotic effect of serotonin. J. Mol. Cell. Cardiol. *52*, 1112-1121.